 doi:10.20944/preprints201806.0167.v1

Articl

Surface removal of copper thin film under the ultrathin water environment for nanoscale process

Junqin Shi [1], Weixiang Peng [1], Juan Chen [1], Liang Fang [1,2,*], Kun Sun [1,*]

[1] State Key Laboratory for Mechanical Behavior of Materials, Xi'an Jiaotong University, Xi'an, 710049, China
[2] School of Mechanical and Electrical Engineering, Xiamen University Tan Kah Kee College, Zhangzhou 363105, P. R. China
* Correspondence: fangl@xjtu.edu.cn; Tel.: +86 29 8266 5479
sunkun@mail.xjtu.edu.cn; Tel.: +86 29 8266 5479

Abstract: The surface planarity and asperity removal behaviors of atomic scale under the ultrathin water environment was studied for the nanoscale process by molecular dynamics simulation. The monolayer atomic removal was achieved under the noncontact and monoatomic layer contact conditions with different water film thickness, and the newly formed surface is relatively smooth and no deformed layer and plastic defects exist. The nanoscale processing is governed by the interatomic adhering action during which the water film transmits the loading forces to Cu surface and thereby result in the migration and removal of surface atoms. With scratching depth ≥ 0.5 nm, the abrasive particle squeezed out the water film from scratching region and scratched Cu surface directly, leading to the surface quality deterioration mainly governed by the plowing action. This study brings the goals of "0 nm planarity, 0 residual defects and 0 polishing pressure" closer to us in the nanoscale process for the development of ultra-precision manufacture technology.

Keywords: Surface removal; Nanoscale process; Copper thin film; Ultrathin water film

1. Introduction

With the rapid development of ultra-precision manufacture technology (UMT) and miniaturized components, chemical mechanical polishing (CMP) technology has been widely applied in the semiconductor industry. Due to the shrinkage of ultralarge scale integrated circuits, new challenges for CMP are created recently, one of which is the low root-mean-square roughness (on the order of subnanometer) [1-4]. The initial requirement of reducing the step-height differences to about 50 nm was changed to 30 nm, then to 10 nm, and now a zero nm difference is desired [5, 6]. Further, the three-"zero" target, namely, "0 nm planarity, 0 defects, and 0 polishing load", is even put forward and desired to be reached by the year 2020 [5]. With this order of size, the removal of polishing material within a few and even only one atomic layers from the film or coating surface is still challenging. In this case, as polishing process has occurred in the local area adjacent to the abrasive particles or cutting tool, wear mechanism must differentiate with macroscopic world. Therefore, it is essential to completely understand the physical/chemical mechanisms of wear underlying the CMP process and develop novel polishing approaches at nanometer scale.

It is known that in CMP process, a major requirement is the complete removal of the overburden materials and coating asperities, with minimal dishing and erosion, as well as minimal levels of surface defects [3]. To make the process efficient, the aqueous slurry, consisting of abrasive particles in a mixture of several chemicals, is used to planarize the wafer surface. Thus, CMP has been proposed to be a comprehensive process with chemical and mechanical synergy, where mechanical wear couple with mechanical corrosion by abrasive particles and chemical corrosion by the slurry solution take place simultaneously [7]. Mechanical wear has been interpreted to be that abrasive particles are indented into polishing substrate surface under pressure and driven to slide on the wafer surface, thereby removing the material.

 doi:10.20944/preprints201806.0167.v1

Regardless of chemical erosion or reaction, the mechanical wear is influenced by many variables in a typical polishing process, such as process parameters including pressure, indentation depth and velocity and other important parameters including the wafer nature, abrasive size, and abrasive geometry, etc. [1, 3, 8-11]. In addition, the slurry is another factor which has a significant effect on the polishing environment and makes the polishing process more complicated [12-14]. As one of the simple but key components in slurry, water not only carries the other components, but also acts as an efficient lubricant which affects the friction and wear behavior of polished surfaces, the material removal rate and the quality of polished surface [15]. By studying the nanoscale friction and wear properties of silicon wafer, Chen et al. found that both the wear rate and friction coefficient in the water lubrication were smaller than that in dry friction conditions, and the wear mechanism of water lubrication was considered to be of molecule-scale removal process [16]. Although the study was concentrating on the synthetic function of chemical and mechanical actions, the results from the study can give us helps in this research to understand the friction and wear behavior of the water-lubricated surface. Ren et al. simulated the AFM-based nanoscratching process with water-layer lubrication by molecular dynamics (MD), and the results indicated that the water layer has a positive impact on the surface quality and a significant influence on the scratching forces (normal forces and tangential forces) [17]. However, to date, the mechanism research of water influencing the polishing behaviors is very limited, for instance, whether the surface or coating asperities will be efficiently removed with minimized damage to the polished surface quality under the noncontact condition as reported by Su [13] and how water interacts with abrasive particle and polished material are still ambiguous, especially for the polishing depth within a few and even only one atomic layers from the surface.

Therefore, we conducted a large scale three-dimensional MD simulation by sliding a diamond particle over copper (Cu) thin film with lubrication of ultrathin water film. The single-circle polishing was represented by the nanoscratching process. Hereinto, the Cu thin film is chosen as the polished material due to that it is now the prior choice for the interconnection in the integrated circuit, because of its highly favorable electrical and electromigration resistance characteristics [3]. Also, because the material deformation, corrosive removal mechanism, surface defects and scratching forces in the scratching process at the subnanometer scale should be different from those at larger scale [4], the various scratching depth less than or equal to 1 nm was adopted, as well as various thickness of water film. This work will be helpful to reveal the role of water in polishing process and understand the friction and wear properties of polished material.

2. Simulation methodology

The MD simulation was performed with LAMMPS code to investigate the atomic removal mechanism of Cu thin film with lubrication of water film. Figure 1 shows the atomistic model of simulation system consisting of a diamond particle, a water film and a defect-free monocrystalline Cu thin film. The spherical abrasive particle constructed with perfect diamond lattice was positioned vertically at a height of 2.0 nm above the water film. Since the abrasive particles in CMP process are usually harder than the machined materials, especially for the relatively soft Cu, it was assumed as ideally rigid body [18]. The water film with density of 1.0 gcm-3 was constructed through Materials Studio software and then transferred to the input file using in LAMMPS code. Atoms of the Cu thin film were initially arranged in a perfect FCC crystalline structure with a lattice constant of a = 0.3615 nm. The Cu thin film was comprised of 656608 atoms with a dimension of 68a×68a×35a along x-[100], y-[010] and z-[001] directions, and contained Newtonian zone, boundary zone and thermostat zone. The boundary atoms at the bottom of the thin film were fixed to reduce the boundary effects, and the thermostat zone was used to imitate the heat dissipation properly. The motion of atoms in Newtonian and thermostat zones obeyed the classical Newton's second law and was integrated through Velocity-Verlet algorithm with a time step of 1 fs. Lateral periodic boundary conditions were imposed and the temperature of 300 K was performed initially in the workpiece. Details of the computational parameters of MD simulations were summarized in Table 1.

Preprints (www.preprints.org) | NOT PEER-REVIEWED | Posted: 12 June 2018 doi:10.20944/preprints201806.0167.v1

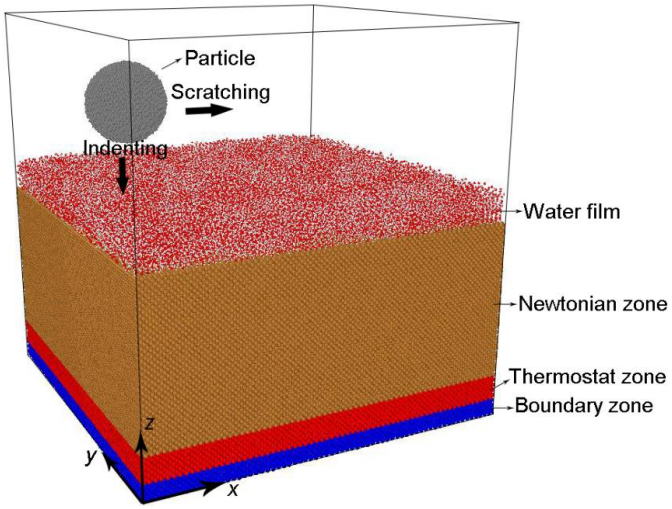

Figure 1. Schematic model of MD simulation system.

The reliability of the simulation results depends on the accuracy of the MD simulation which is governed by the interaction potential. Interatomic forces within the Cu are derived from the embedded atom method (EAM) potential, which provides a more realistic description of metallic cohesion and avoiding ambiguity inherited by the volume dependency [19]. The Morse potential [20] was adopted to depict the Cu-C interaction with potential parameters expressed in Table 1. The C-C interaction was omitted because of the treatment of rigid body. The rigid TIP4P model [21, 22] was applied to simulate the condensed phase of water film. The interactions of H atoms in water molecules with other types of atoms were neglected due to the weak influence of H atoms [17]. The Cu-O and C-O interactions were described by Lennard-Jones (12-6) potential and the relevant parameters were obtained by Lorentz-Berthelot mixing rules [17, 23] as shown in Table 1.

Table 1. Parameters used in the MD simulations.

Properties	**Parameters**
Abrasive particle	Diamond, sphere with radius of 2.5 nm, 11976 atoms
Water film	Density of 1.0 gcm^{-3}, thickness (H): 0.3, 0.5 and 1.0 nm
Workpiece	Cu (FCC), 68a×68a×35a (a=0.3615 nm), 656608 atoms
Potential for Cu thin film	EAM potential: $E_i = F_\alpha\left(\sum_{j\neq i}\rho_\beta\left(r_{ij}\right)\right)+\frac{1}{2}\sum_{j\neq i}\phi_{\alpha\beta}\left(r_{ij}\right)$
Potential for particle-Cu film	Morse potential: $E = D_0\left[e^{-2\alpha(r-r_0)}-2e^{-\alpha(r-r_0)}\right]\ \ r<r_c$ where D_0=0.1 eV, α=1.7 nm^{-1} and r_0=0.22 nm
Potential for water molecules	O–O, ε=0.1554 kcal/mol, δ=0.31655 nm
Potential for water–particle	O–C, ε=0.1 kcal/mol, δ=0.3275 nm
Potential for water–workpiece	O–Cu, ε=0.2708 kcal/mol, δ=0.28877 nm
Scratching	Depth: -0.2, 0.1, 0.5, 1.0 nm; distance: 9.0 nm; v = 10 ms^{-1}

MD simulations of the nanoscratching process consisted of three stages: (i) relaxation process of 50 ps, implemented to optimize system energy at NVT ensemble with the Nose–Hoover thermostat which has been commonly used as one of the most accurate and efficient methods for

 doi:10.20944/preprints201806.0167.v1

constant-temperature MD simulations; (ii) nanoindentation, during which the particle moved downward and penetrated into the substrate along –z direction; and (iii) nanoscratching, the abrasive particle moved along x direction at the constant indentation depth. It modeled the mechanical abrasion and planarization of the monocrystalline Cu surface, as may be the case in the CMP process. Displacement-controlled method with velocity of 10 ms-1 was used to keep the movement of particle at the nanoindentation and nanoscratching stages. The NVE ensemble with the Langevin thermostat was used to control the temperature of thermostat layer and water film. The various water film thickness (0, 0.3, 0.5 and 1.0 nm) and scratching depth (-0.2, 0.1, 0.5 and 1.0 nm) were used to reveal the effect of water film thickness on the atomic removal behaviors, as shown in Table 1. The dislocation extraction algorithm [24, 25] was used to identify dislocation defects by converting all identified dislocations into continuous lines and computing their Burgers vectors in a fully automated fashion. The open visualization tool (Ovito) [26] was used to visualize the simulation results.

3. Results and discussions

It has been approved by increasingly more researchers that the scratching depth during CMP can be in the order of subnanometer. For example, the indentation depth of a particle with diameter of 50 nm analyzed by Luo and Dornfeld [1, 27] was around 0.07 nm in CMP process. At the scratching depth of subnanometer, the polishing behaviors should be different from those with relatively large depth [4]. Thus, in order to reveal the physical essence underlying CMP process, we adopted four scratching depth of -0.2, 0.1, 0.5 and 1.0 nm to study the interactions among particle, water film and Cu thin film. Here, the scratching depth is defined as the distance that the surface atoms of particle penetrate into Cu surface, the negative value -0.2 nm indicates that the particle does not penetrate into Cu substrate, meaning there exists a noncontact between particle and polished surface, and the value 0.1 corresponds to the monoatomic layer contact.

Figure 2 shows the worn morphology of the cross-sectional views of xz plane and the plane views of xy plane where the surface atoms in yellow color are only displayed and the water film with 1.0 nm thickness is omitted, and Figure S1 (in the Supporting Information) shows the slice configuration with 0.5 nm thickness in xz plane. In Figure 2(a), it can be seen that in the scratching region, a new surface layer appeared on the initial subsurface of Cu thin film after the particle passed by, and some initial surface atoms were lifted above the Cu surface. Figure S1(a) indicates that many surface atoms were removed from their original positions, leading to the formation of vacancy on the surface as shown from the plane views. Therefore, it is thought that one monoatomic layer was removed from the initially perfect Cu substrate at the scratching depth of -0.2 nm. This way of monolayer material removal also occurred at the scratching depth of 0.1 nm as shown in Figure 2(b) and Figure S1(b). The newly formed surface is not very flat in the local scratching region under the monoatomic layer contact condition. However, the step-height difference in the whole scratching region is relatively close to uniformization within one monoatomic layer, as shown in the cross-sectional views in Figure 2(a, b). This suggests that the polishing quality of Cu surface is very close to the target of “0 nm planarity” under the noncontact or monoatomic surface contact conditions. The removed Cu atoms are in monoatomic form or cluster formed by a few atoms, as shown in the inset, which is consistent with the removal of silicon atoms with indentation depth of 0.1 nm as reported in Ref [4]. In the real CMP process, the slurry and water are continuously flowing due to the pad rotation, so the removed material in the aforementioned form are taken away quickly [28].

Preprints (www.preprints.org) | NOT PEER-REVIEWED | Posted: 12 June 2018 doi:10.20944/preprints201806.0167.v1

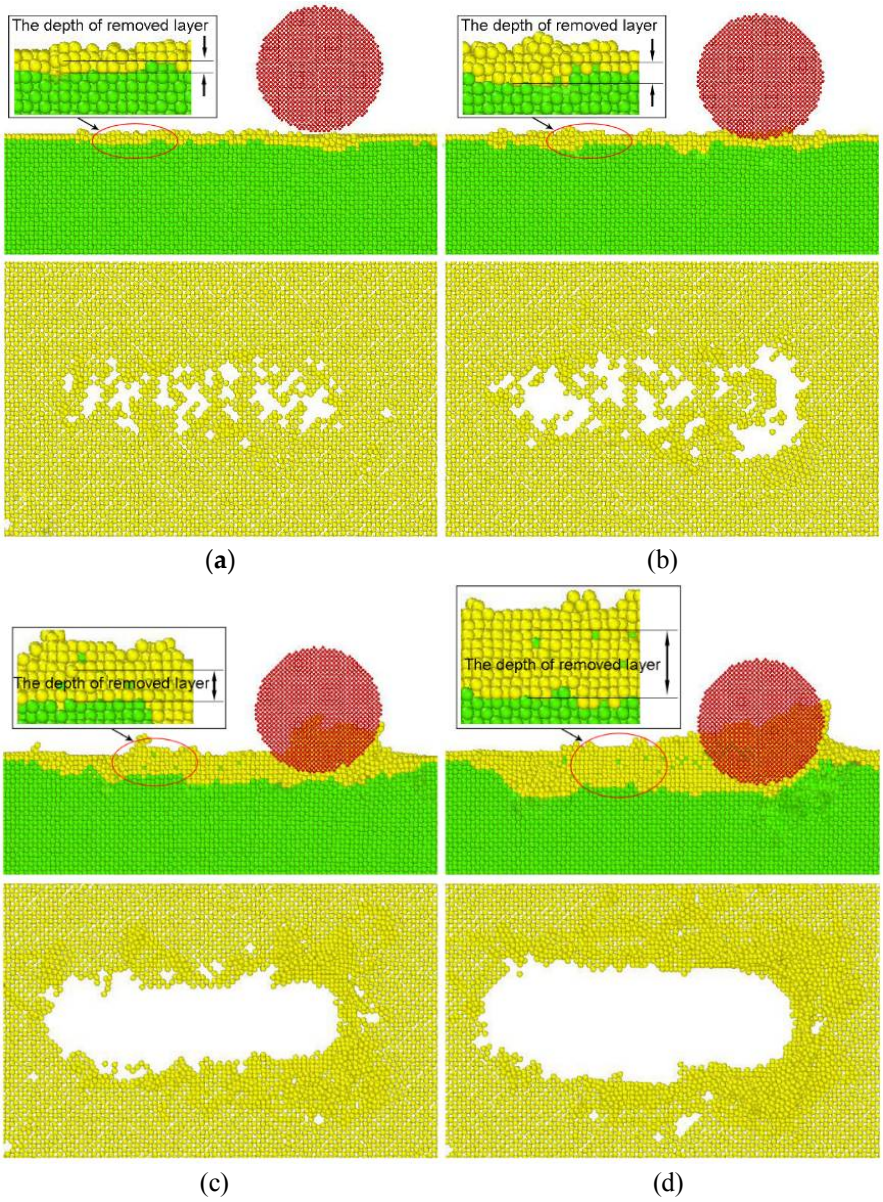

Figure 2. Snapshots of worn morphology of the cross-sectional views of xz plane and the plane views of xy plane with omission of water film of 1.0 nm thickness, under various scratching depth (h): (a) -0.2 nm, (b) 0.1 nm, (c) 0.5 nm and (d) 1.0 nm, at a scratching distance of 9 nm. Color code: yellow, surface Cu atoms; green, other Cu atoms; red, abrasive particle.

Figure 2(c, d) shows the worn morphology with scratching depth up to 0.5 and 1.0 nm. It is clear that due to the increase of scratching depth, the abrasive particle contacted more Cu atoms and thereby resulted in a larger removed zone, and almost all of the surface Cu atoms contacting with particle were removed during scratching process (as shown in Figure S1(c, d)). As the particle moved forward, a large number of deformed atoms accumulated to form clusters or chips ahead of the particle, and meanwhile, the remarkable ridges (i.e. pile-up of atoms) along both the left and right sides of particle were produced, especially at the scratching depth of 1.0 nm as shown in Fig S2 (in the Supporting Information). After the particle passed by, a groove was formed. These results are in well agreement with the dry nanoscratching process as shown in Fig S1(c), as well as the AFM-based nanoscratching process with water-layer lubrication [17]. Observed from the distribution of surface Cu atoms in yellow color in the cross-sectional views, the bottom of groove shows obviously atomic steps and the ridge is non-uniform in height. Also, although the removal rate of surface atmos increased obviously with the scratching depth increasing to 0.5 and 1.0 nm, the height difference between groove and ridge dramatically increased, indicating that the large

Preprints (www.preprints.org) | NOT PEER-REVIEWED | Posted: 12 June 2018 doi:10.20944/preprints201806.0167.v1

scratching depth leads to the damage of surface quality. This is in contrast with the case of small scratching depth of -0.2 and 0.1 nm, where just a monoatomic layer was removed, and no obvious groove and ridge was formed, as shown in Figure 2(a, b) and Figure S1(a, b).

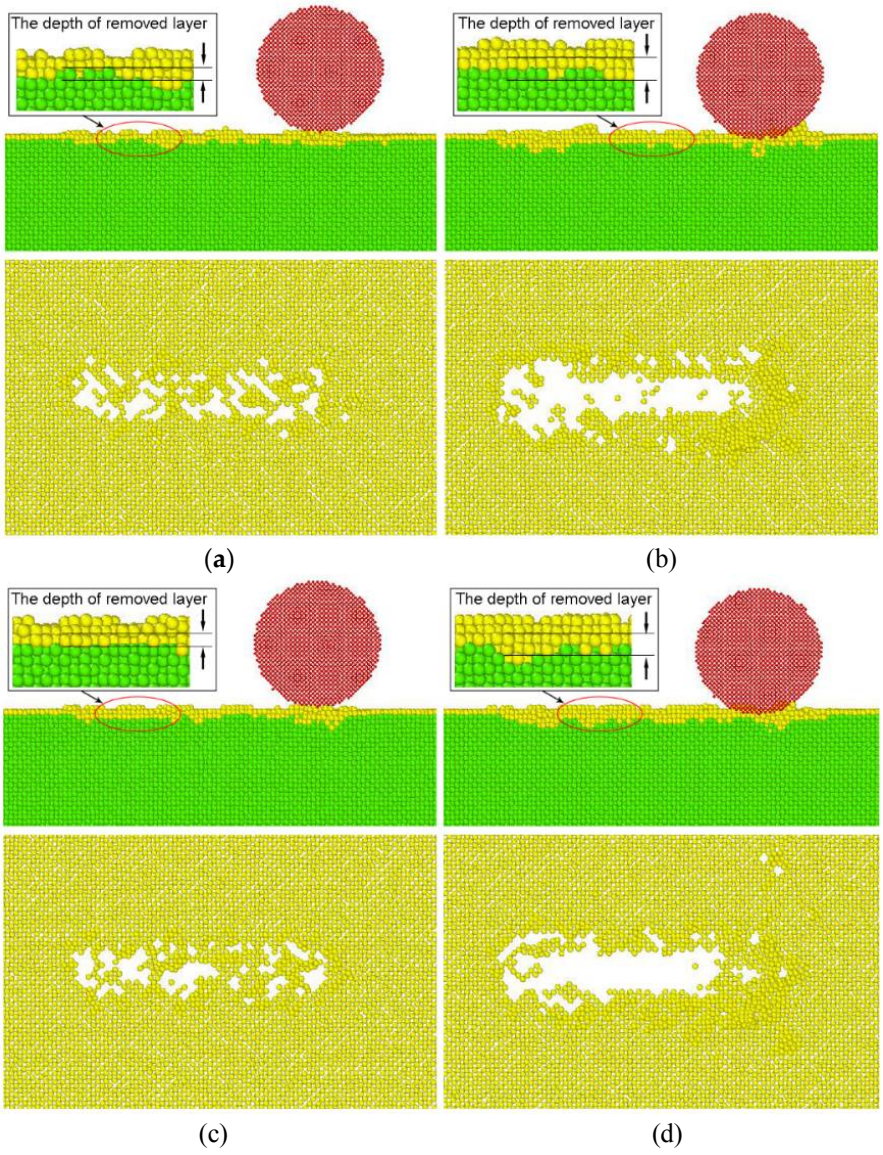

Figure 3. Snapshots of worn morphology of the cross-sectional views of xz plane and the plane views of xy plane with omission of water film, under various water film thickness (H) and scratching depth (h), H=0.5 nm: (a) h=-0.2 nm, (b) h=0.1 nm; H=0.3 nm: (c) h=-0.2 nm, (d) h=0.1 nm.

To evaluate the effect of water film thickness on the removal process and surface quality, we also conducted MD simulations of nanoscratching process under the water film thickness of 0.3 and 0.5 nm approximately corresponding to the monolayer and bilayer water film, as well as dry nanoscratching. The snapshots of worn morphology are displayed in Figure 3, Figure S3 and Figure S4 (in the Supporting Information). Figure 3 and Figure S3 indicate that a one-atom-thin layer was removed after scratching under different scratching depth and water film thickness, which is almost the same with the simulated results under the water film thickness of 1.0 nm in Figure 2(a, b). For the dry nanoscratching in Figure S4, the monoatomic layer removal just occurred at scratching depth of 0.1 nm, whereas the Cu surface still maintained its perfect lattice structure at scratching depth of -0.2 nm due to the weak interaction between particle and Cu substrate. Comparing the plane views in Figure 2(a, b), Figure 3 and Figure S4(b), it can be seen that, on the one hand, the surface vacancy formed by the atomic removal in the scratching region becomes more obvious as the water film thickness decreases from 1.0 nm to 0 nm, indicating that the number of removed atoms in the central

 doi:10.20944/preprints201806.0167.v1

region of scratching increases with the decrease of water film thickness; however, on the other hand, the area of scratching region slightly decreases with the decrease of water film thickness under the same scratching depth.

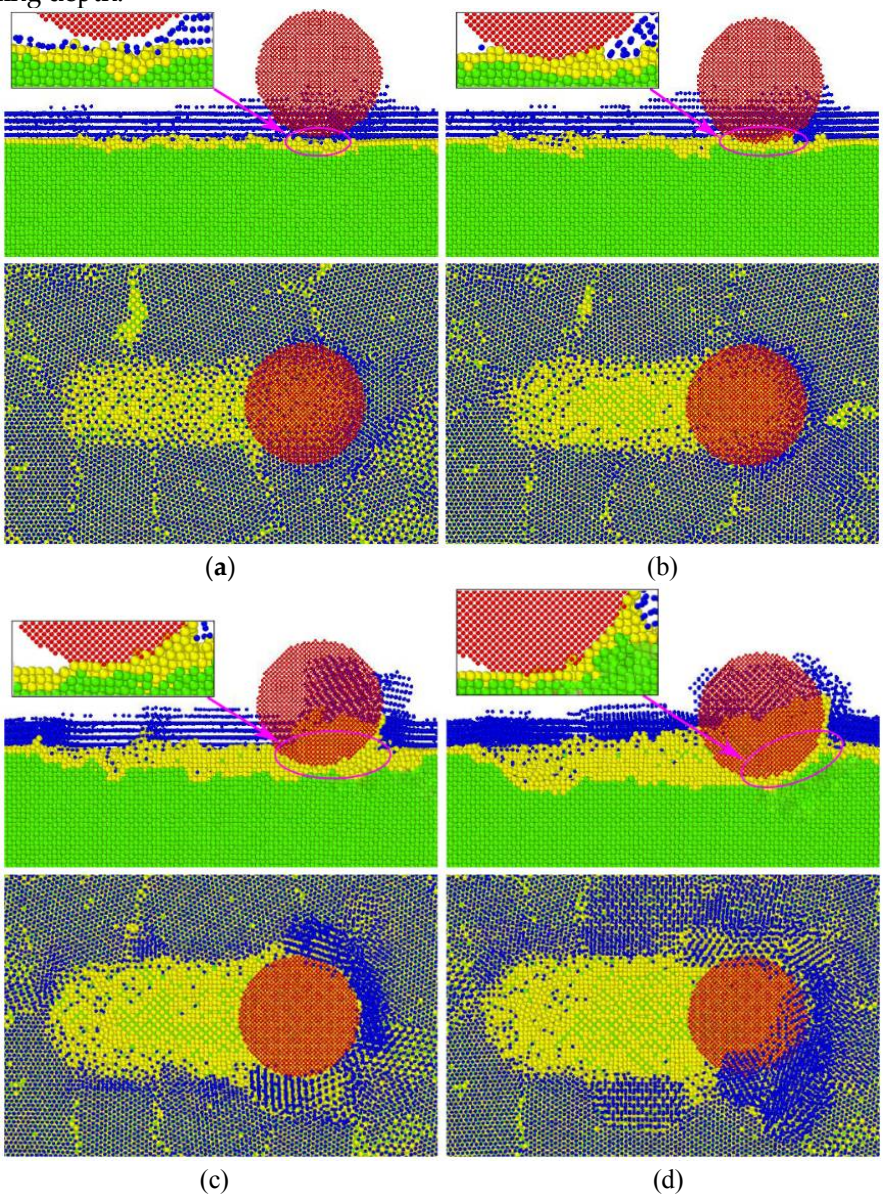

Figure 4. Snapshots of worn configuration of the cross-sectional views of xz plane and the plane views of xy plane under various scratching depth (h): (a) -0.2 nm, (b) 0.1 nm, (c) 0.5 nm and (d) 1.0 nm, at a scratching distance of 9 nm, with water film thickness of 1.0 nm. The blue represents oxygen atoms in water molecules.

Further, to reveal the mechanism of material removal, the worn configurations with the presence of water film and the local interaction zones were extracted and shown in Figure 4, and the number of water molecules remaining in the scratching region was calculated in Figure 5. In Figure 4, there are a small number of water molecules accumulating in front of particle as the scratching depth is -0.2 and 0.1 nm, while the number of accumulated water molecules increases considerably with the scratching depth up to 0.5 and 1.0 nm. In contrary, the number of water molecules remaining in the scratching region decreases dramatically, as displayed in the plane views in Figure 4 and Figure 5. Particularly, the number of water molecules under noncontact condition is about quadruple that at scratching depth of 0.1 nm, but no major difference in the wear of Cu thin film is observed as mentioned above. This indicates these water molecules remaining in the scratching

Preprints (www.preprints.org) | NOT PEER-REVIEWED | Posted: 12 June 2018 doi:10.20944/preprints201806.0167.v1

region played a predominant role at shallower scratching depth during the monoatomic layer removal.

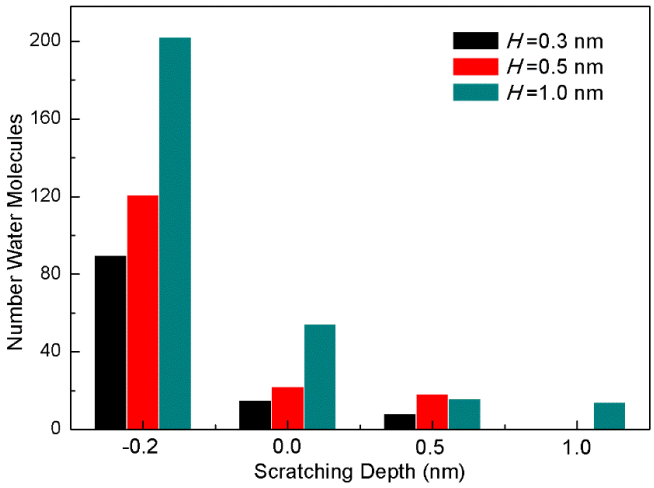

Figure 5. Number of water molecules within groove region at various scratching depth and water film thickness.

For the scratching process of noncontact condition (the scratching depth of -0.2 nm) with water film thickness of 1.0 nm, the cross-sectional view in Figure 4(a) shows that the space between particle and Cu surface is occupied by a large number of remaining water molecules. The average interaction forces listed in Table 2 manifest that the interactive force of particle-Cu film (0.18 nN) is much less than the interactive forces of both water-Cu (41.52 nN) and water-particle (46.08 nN). These results indicate the monoatomic layer removal should be ascribed to the water-Cu interactive force. Figure 6 displays the atomic removal process at different simulation time, where the three oxygen atoms and Cu atoms around the blue Cu atom were marked with other colors. The Cu surface beneath particle shows a slight deformation because water molecules beneath particle can transmit the force from the loading of particle to Cu surface. From 5 ps to 15 ps and then to 35 ps, the blue Cu atom was gradually pushed or attracted by the water molecules (oxygen atoms marked with purple and light blue). Once the water-Cu interactive force was larger than the force that is enough to break the metallic bond of Cu, the Cu atoms were removed from their initial positions and even adhered to the particle. For instance, the position of the blue Cu atom was higher than the original Cu surface at 100 ps, as shown in Figure 6(d). This kind of removal behavior continuously occurred in the nanoscratching process. In this process, the adhesion and removal of surface atoms just cause the surface structure change, resulting in surface roughness on the order of atomic size magnitude which is consistent with other research [1, 4, 27]. A similar removal behavior of surface atoms was also occurred in the scratching process with scratching depth of 0.1 nm; meanwhile, the adhering action of Cu atoms to particle increases obviously, which is validated by the interactive force of particle-Cu (18.44 nN), thus leading to the increase of removed atoms and the area of scratching region as shown in Figure 2(b). Moreover, the monocrystalline Cu substrate was divided into several zones marked with different colors in Figure 7. It can be seen from the circle A in Figure 7(b) that some dispersive Cu atoms or small atom clusters were shifted from their original positions in zone 2 and zone 5 and then appeared in zone 3 and zone 6, but no chips or debris were observed. Less atom shift occurred at scratching depth of -0.2 nm in Figure 7(a). These results provide more sufficient evidence manifesting that the surface atoms are removed by the adhering action (Figure 6) under the noncontact and monoatomic layer contact conditions during CMP process.

Preprints (www.preprints.org) | NOT PEER-REVIEWED | Posted: 12 June 2018 doi:10.20944/preprints201806.0167.v1

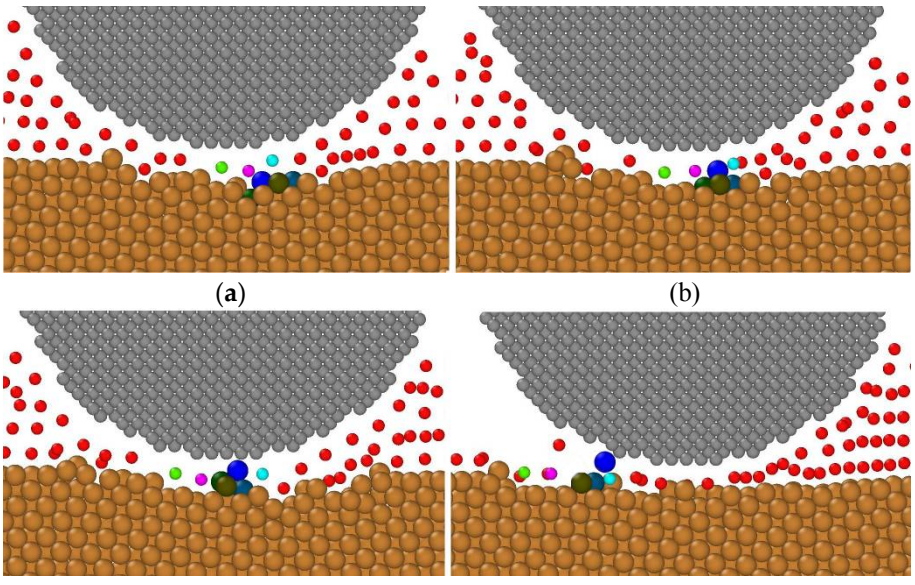

Figure 6. Snapshots of atomic removal process within 5 nm slice of the scratching central region, at different simulated time: (a) 5 ps, (b) 15 ps, (c) 35 ps and (d) 100 ps. Color code: red, oxygen atoms in water molecule; gray, abrasive particle; dark yellow, Cu atoms.

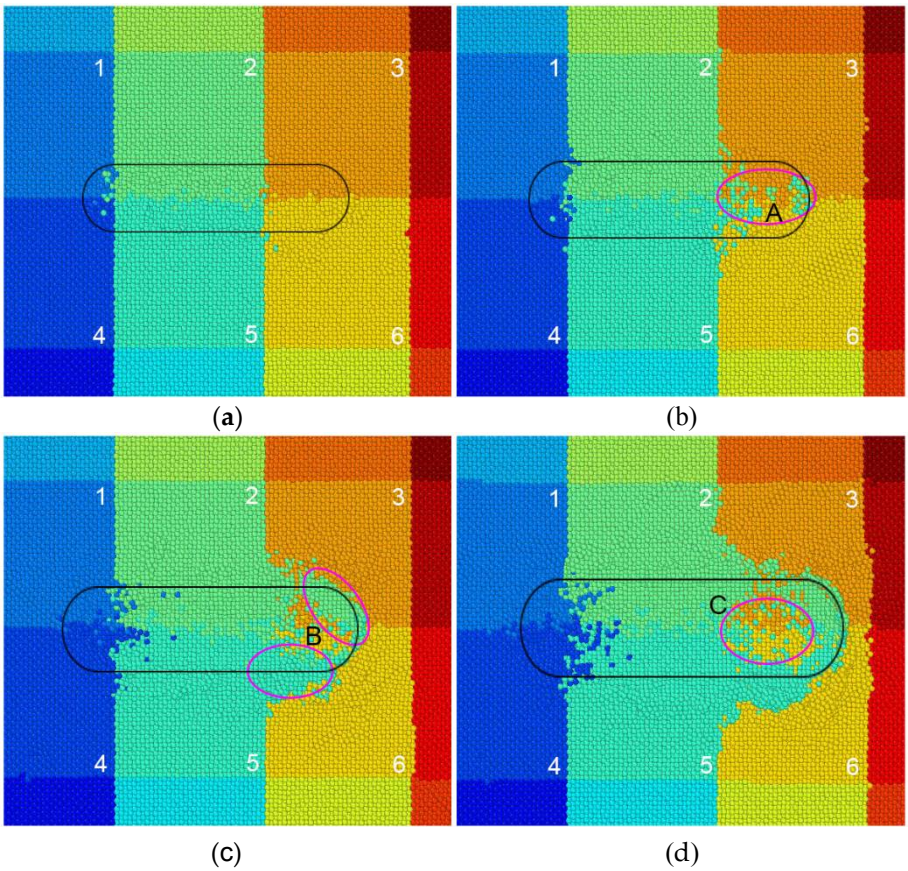

Figure 7. Snapshots of worn configuration of the cross-sectional views of xz plane for various scratching depth (h): (a) -0.2 nm, (b) 0.1 nm, (c) 0.5 nm, (d) 1.0 nm, at a scratching distance of 9 nm, with water film thickness of 1.0 nm. The black line marks the scratching contour.

As the scratching depth increased to 0.5 and 1.0 nm, the most of water molecules under particle were squeezed out of the scratching region (as proved by the number of water molecules in Figure 5), and the particle contacted with Cu surface directly, as displayed in Figure 4(c, d). The interactive

Preprints (www.preprints.org) | NOT PEER-REVIEWED | Posted: 12 June 2018 doi:10.20944/preprints201806.0167.v1

forces of water-Cu and water-particle decrease rapidly while that of particle-Cu increases dramatically (in Table 2). Especially, at the scratching depth of 1.0 nm, the interactive force of particle-Cu (147.98 nN) becomes much larger than the other two forces (4.24 and 13.12 nN), but very close to the interactive force of particle-Cu (158 nN) for dry nanoscratching, which suggests that the direct interaction between abrasive particle and Cu thin film predominantly governs the material removal. This is contrary to that occurring at the scratching depth less than or equal to 0.1 nm. During the moving forward of particle, one amorphous layer was formed; the deformation zone in the Cu film became larger, and several chips or debris were generated in front of the particle, as shown in Figure 7(c, d). Meanwhile, a fraction of Cu atoms were shifted from their original positions in zone 2 and zone 5 and dispersed underneath the particle in zone 3 and zone 6, as enclosed in circle C in Figure 7(d). Therefore, it is thought that the surface atoms are mainly removed by the ploughing action and a small fraction of adhering also occurs at the large scratching depth. The ploughing leads to that the structural changes of the Cu thin film are not only near the surface but also in the deep region. The surface quality is deteriorated with larger surface roughness as shown in Figure 2(c, d) and Figure 4(c, d).

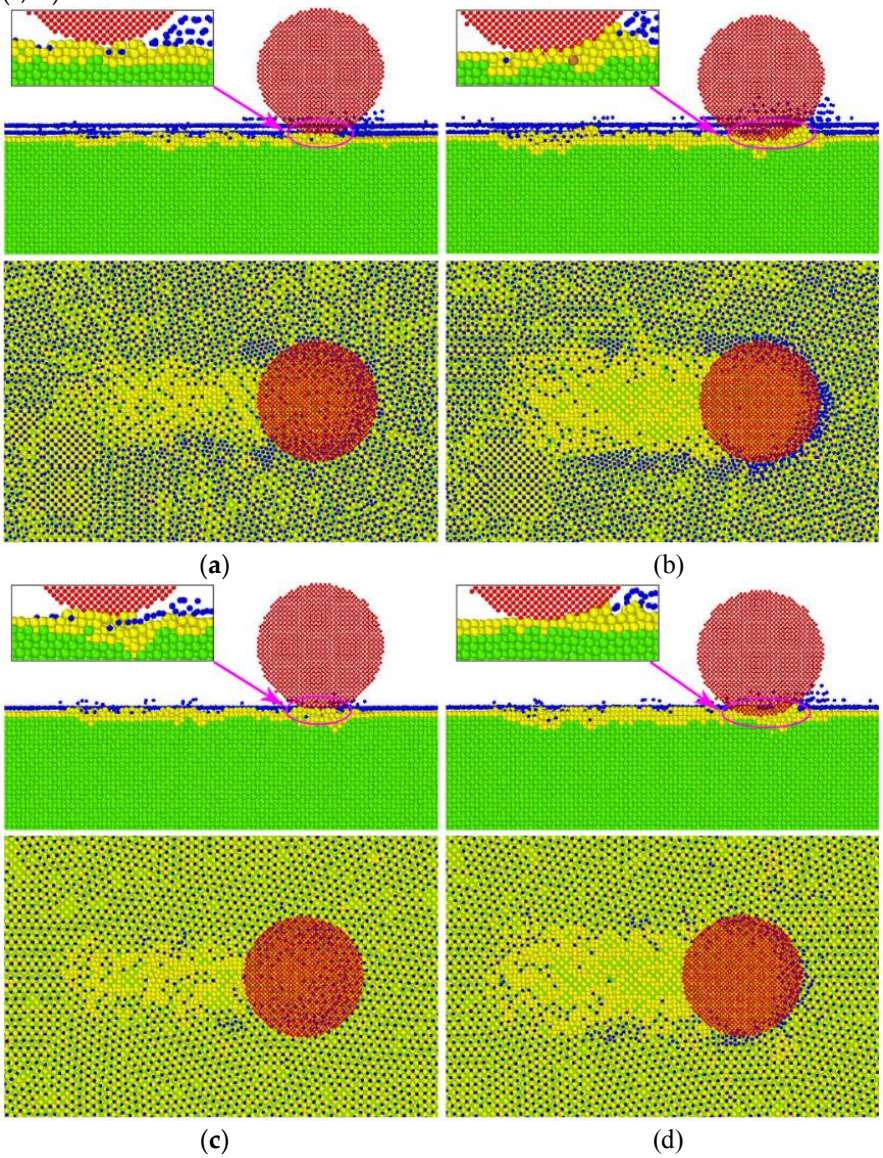

Figure 8. Snapshots of worn configuration of the cross-sectional views of xz plane and the plane views of xy plane under various water film thickness (H) and scratching depth (h), H=0.5 nm: (a) h=-0.2 nm, (b) h=0.1 nm; H=0.3 nm: (a) h=-0.2 nm, (b) h=0.1 nm.

Figure 8 shows the nanoscratching results with monolayer and bilayer water film. It is clear that

 doi:10.20944/preprints201806.0167.v1

the distribution of water molecules around particle at both two scratching depth (-0.2 and 0.1 nm) is similar to that under the water film thickness of 1.0 nm (in Figure 4(a, b)). Whereas, the number of water molecules remaining in the scratching region decreases further with the decrease of water film thickness from 1.0 nm to 0.3 nm, as validated by the number in Figure 5. The insets in Figure 8(a, c) show that some water molecules still remained beneath particle and more water molecules existed in the space ahead of particle. All those water molecules played an important role in facilitating the removal of monoatomic layer. Contrarily, with scratching depth increasing to 0.1 nm in Figure 8(b, d), there were only a small number of water molecules remaining beneath particle, and thus the particle started to contact with surface Cu atoms, similar to the dry nanoscratching in Figure S4(b). The average interaction forces in Table 2 indicate that the interactive forces of water-Cu and water-particle decrease but the particle-Cu interactive force increases slightly with the water film thickness decreasing to 0.5 and 0.3 nm. For example, at the scratching depth of 0.1 nm, as the water film thickness decreases from 1.0 nm to 0.5 nm and then to 0.3 nm, the interactive force of water-Cu decreases from 39.44 nN to 16.28 nN and then to 10.41 nN; however, the interactive forces of particle-Cu are 18.44, 20.12 and 21.96 nN, respectively. Clearly, the interactive force of particle-Cu becomes comparable with and even larger than twice the interactive force of water-Cu under water film thickness of 0.5 and 0.3 nm, respectively. These results indicate the contribution of water film to the removal of monoatomic layer decreases, but the adhering action of Cu atoms to abrasive particle increases under thinner water film.

Table 2. Average interaction forces along scratching direction.

Water film thickness /nm	Scratch depth /nm	Water-Cu interaction /nN	Water-particle interaction /nN	Particle-Cu interaction /nN
0.3	-0.2	7.70	9.24	1.23
	0.1	10.41	11.26	21.96
	0.5	4.48	5.40	86.94
0.5	-0.2	17.29	16.17	0.73
	0.1	16.28	17.80	20.12
	0.5	7.02	6.52	90.08
1.0	-0.2	41.52	46.08	0.18
	0.1	39.44	51.94	18.44
	0.5	19.98	30.69	95.59
	1.0	4.24	13.12	147.98

As well known, a major requirement for the CMP process is the minimal dishing and erosion, as well as minimal levels of surface defects [3]. Further, approaching and even achieving the three-"zero" target of "0 nm planarity, 0 defects, and 0 polishing load" are the desired goals for CMP technology [5]. Hence, it is important to evaluate the surface defect of Cu thin film. All the aforementioned results indicate that the monolayer removal can be achieved under the noncontact and monoatomic layer contact conditions with different water film thickness, and the surface quality becomes better under thicker water film. With the scratching depth increasing to 0.5 and 1.0 nm, an obvious groove with ridge along the both sides is formed, and chips or debris are produced and accumulated in front of particle. They increase the surface roughness and thereby lead to the deterioration of the surface quality. Moreover, the dislocation length was extracted and shown in Table 3 to evaluate the plastic deformation within Cu thin film. It can be seen that at the scratching depth of -0.2 and 0.1 nm, no dislocations were activated in the scratching process under different water film thickness. These results are consistent with experimental results [4, 5], which indicated that a well ordered crystalline surface could be clearly seen in the CMP generated subsurface, and no

 doi:10.20944/preprints201806.0167.v1

damaged layers are found. However, the increase of scratching depth induced the nucleation and propagation of dislocations, for instance, the dislocation length increased dramatically from 28.57 nm to 108.01 nm as the scratching depth increased from 0.5 nm to 1.0 nm. Also, because the thickening of water film decreases the interaction force between the rigid particle and Cu surface (Table 2), leading to the decrease of the stress acting on Cu thin film, the dislocation length decreases as listed in Table 3.

Table 3. Dislocation length within monocrystalline Cu.

Water film thickness /nm	0.3			0.5			1.0			
Scratch depth /nm	-0.2	0.1	0.5	-0.2	0.1	0.5	-0.2	0.1	0.5	1.0
Dislocation length /nm	0	0	65.55	0	0	42.33	0	0	28.57	108.01

4. Conclusions

In this work, the MD simulation was applied to investigate the effect of scratching depth on the atomic-scale removal behaviors of Cu thin film under the ultrathin water environment. The results indicate that the monoatomic layer removal can be achieved under the noncontact and monoatomic layer contact conditions, the new surface is relatively smooth and no deformed layer and plastic defects exist on the subsurface and within Cu film. During the nanoscale processing, the removal of monoatomic layer is governed by the interatomic adhering action, namely, the water film can transmit the forces from the loading of abrasive particle to Cu surface and thereby result in the migration and then removal of surface atoms. However, with the scratching depth increasing to 0.5 and 1.0 nm, the particle interacts with Cu substrate directly and the water film beneath particle can be easily squeezed out of the scratching region. This scratching process leads to the formation of an obvious groove and ridge along the both sides of groove, the accumulation of a large number of chips ahead of particle, and the generation of dislocations within monocrystalline Cu. Therefore, the surface atoms are mainly removed by the plowing action of abrasive particle, which increases the surface roughness and thereby leads to the deterioration of the wafer quality. It is known that for refined coatings or devices with nodes of 5 nm or smaller, a zero nm planarity, zero residual defects and, possibly, zero polishing pressure are required. This study indicates that it is possible to bring the goals closer to us although we cannot achieve the goals immediately.

5. Patents

Supplementary Materials: The following are available online at www.mdpi.com/xxx/s1, Figures S1 to S4 containing snapshots of worn morphology at scratching depth of -0.2, 0.1, 0.5 and 1.0 nm under water film thickness of 1.0, 0.5 and 0.3 nm and the case of no water, snapshots of ridge morphology.

Author Contributions: Conceptualization, Liang Fang and Kun Sun; Investigation, Junqin Shi; Writing-Original Draft Preparation, Junqin Shi; Data analysis, Junqin Shi, Juan Chen and Weixiang Peng.

Funding: This work was supported by the National Natural Science Foundation of China [Grant numbers 51375364, 51475359] and the Natural Science Foundation of Shaanxi Province of China [2014JM6219].

Conflicts of Interest: The authors declare no conflict of interest. The funders had no role in the design of the study; in the collection, analyses, or interpretation of data; in the writing of the manuscript, and in the decision to publish the results.

References

1. Luo, J. F.; Dornfeld, D. A.; Material Removal Mechanism in Chemical Mechanical Polishing: Theory and Modeling. *IEEE T. Semiconduct. M.* **2001**, *14*, 112–133.
2. Kasai, T.; Bhushan, B. Physics and tribology of chemical mechanical planarization. *J. Phys.: Condens. Matter* **2008**, *20*, 225011.
3. Lu, Z. Y., Lee, S. H.; Babu, S.V.; Matijevic, E. The use of monodispersed colloids in the polishing of copper and tantalum. *J. Colloid Interf. Sci.* **2003**, *261*, 55–64.
4. Si, L. N.; Guo, D.; Luo, J. B.; Lu, X. C. Monoatomic layer removal mechanism in chemical mechanical polishing process: A molecular dynamics study. *J. Appl. Phys.* **2010**, *107*, 064310.
5. Tsujimura, M. The way to zeros: the future of semiconductor device and chemical mechanical polishing technologies. *J. Appl Phys.* **2016**, *55*, 06JA01.
6. ITRS Road Map, 2013, Edition Interconnect, Figure INTC30 Brief History of Planarization Solutions, p. 50.
7. Kaufman, F. B.; Thompson, D. B.; Broadie, R. E.; Jaso, M. A.; Guthrie, W. L.; Pearson, D. J.; Small, M. B. Chemical-mechanical polishing for fabricating patterned W metal features as chip interconnects. *J. Electrochem. Soc.* **1991**, *138*, 3460.
8. Zhao, D. W.; Wang, T. Q.; He, Y. Y.; Lu, X. C. Effect of zone pressure on wafer bending and fluid lubrication behavior during multi-zone CMP process. *Microelectron. Eng.* **2013**, *108*, 33–38.
9. Hung, T. C.; Chang, S. H. Lin, C. C. Su, Y. T. Effects of abrasive particle size and tool surface irregularities on wear rates of work and tool in polishing processes. *Microelectron. Eng.* **2011**, *88*, 2981–2990.
10. Ilie, F. Tribochemical interaction between nanoparticles and surfaces of selective layer during chemical mechanical polishing. *J. Nanopart. Res.* **2013**, *15*, 1997.
11. Zhu, P. Z.; Hu, Y. Z.; Ma, T. B.; Wang, H. Molecular dynamics study on friction due to ploughing and adhesion in nanometric scratching process. *Tribology Letters* **2011**, *41*, 41–46.
12. Luo, Q.; Campbell, D. R.; Babu, S. V. Stabilization of Alumina Slurry for Chemical− Mechanical Polishing of Copper. *Langmuir* **1996**, *12*, 3563–3566.
13. Su, Y. T. Investigation of Removal Rate Properties of a Floating Polishing Process. *J. Electrochem. Soc.* **2000**, *147*, 2290–2296.
14. Patri, U. B.; Pandija, S.; Babu, S. V. Role of molecular structure of complexing/chelating agents in copper CMP slurries. *Mater. Res. Soc. Symp. Proc.* **2005**, *867*, W1.11.
15. Barthel, A. J.; Ala' Al-Azizi; Surdyka, N. D.; Kim, S. H. Effects of gas or vapor adsorption on adhesion, friction, and wear of solid interfaces. *Langmuir* **2014**, *30*, 2977–2992.
16. Chen, X. C.; Zhao, Y. W.; Wang, Y. G. Zhou, H. L.; Ni, Z. F.; An. W. Nanoscale friction and wear properties of silicon wafer under different lubrication conditions. *Appl. Surf. Sci.* **2013**, *282*, 25–31.
17. Ren, J.; Zhao, J.; Dong, Z.; Liu, P. Molecular dynamics study on the mechanism of AFM-based nanoscratching process with water-layer lubrication. *App. Surf. Sci.* **2015**, *346*, 84–98.
18. Chen, Y; Li, Z. N.; Miao, N. M. Polymethylmethacrylate (PMMA)/CeO2 hybrid particles for enhanced chemical mechanical polishing performance. *Tribol. Int.* **2015**, *82*, 211–217.
19. Mishin, Y.; Mehl, M. J.; Papaconstantopoulos, D. A.; Voter, A. F.; Kress, J. D. Structural stability and lattice defects in copper: Ab initio, tight-binding, and embedded-atom calculations. *Phys. Rev. B* **2001**, *63*, 224106.
20. Morse, P. Diatomic molecules according to the wave mechanics. II. Vibrational levels. *Phys. Rev.* **1929**, *34*, 57–64.
21. Khan, H. M.; Kim, S. G. On the wear mechanism of thin nickel film during AFM based scratching process using molecular dynamics. *J. Mech. Sci. Technol.* **2011**, *25*, 2111–2120.
22. Abascal, J. L. F.; Vega, C. A general purpose model for the condensed phases of water: TIP4P. *J. Chem. Phys.* **2005**, 123, 234505.
23. Shi, J. Q.; Zhang, Y. N.; Sun, K.; Fang. L. Effect of water film on the plastic deformation of monocrystalline copper. *RSC Adv.* **2016**, *6*, 96824–96831.
24. Gao, Y.; Ruestes, C. J.; Urbassek, H. M. Nanoindentation and nanoscratching of iron: Atomistic simulation of dislocation generation and reactions. *Comp. Mater. Sci.* **2014**, *90*, 232–240.
25. Stukowski, A.; Albe, K. Extracting dislocations and non-dislocation crystal defects from atomistic simulation data. *Model. Simul. Mater. Sci. Eng.* **2010**, *18*, 085001.
26. Stukowski, A. Visualization and analysis of atomistic simulation data with OVITO–the open visualization tool. *Model. Simul. Mater. Sci. Eng.* **2010**, *18*, 015012.

 doi:10.20944/preprints201806.0167.v1

27. Luo, J. F.; Dornfeld, D. A. Material removal regions in chemical mechanical planarization for submicron integrated circuit fabrication: coupling effects of slurry chemicals, abrasive size distribution,and wafer-pad contact area. *IEEE Trans. Semicond. Manuf.* **2003**, *16*, 45.
28. B. Shiari, R. E. Miller, D. D. Klug. Multiscale simulation of material removal processes at the nanoscale. *J. Mech. Phys. Solids* **2007**, *55*, 2384.